land

MDPI

Article

Modelling Multi-Scenario Ecological Network Patterns and Dynamic Spatial Conservation Priorities in Mining Areas

Wanqiu Zhang [1], Zeru Jiang [2], Huayang Dai [1], Gang Lin [3,4,5,*], Kun Liu [6,*], Ruiwen Yan [1] and Yuanhao Zhu [1]

[1] College of Geoscience and Surveying Engineering, China University of Mining and Technology—Beijing, Beijing 100083, China; bqt2200204006t@student.cumtb.edu.cn (W.Z.); dhy@cumtb.edu.cn (H.D.); yanruiwen819@hotmail.com (R.Y.); bqt2100204050@student.cumtb.edu.cn (Y.Z.)
[2] School of Government, Peking University, Beijing 100871, China; jiangzeru@pku.edu.cn
[3] Institute of Geographic Science and Natural Resources Research, Chinese Academy of Sciences, Beijing 100101, China
[4] College of Resources and Environment, University of Chinese Academy of Sciences, Beijing 100049, China
[5] Key Laboratory of Coupling Processes and Effects of Natural Resource Elements, Ministry of Natural Resources, Beijing 100055, China
[6] Land Satellite Remote Sensing Application Center, Ministry of Natural Resources, Beijing 100048, China
* Correspondence: ling@lreis.ac.cn (G.L.); liukun@lasac.cn (K.L.)

Abstract: Mining activities have significantly altered the land use patterns of mining areas, exacerbated the degree of landscape fragmentation, and thereby led to the loss of biodiversity. Ecological networks have been recognized as an essential component for enhancing habitat connectivity and protecting biodiversity. However, existing studies lack dynamic analysis at the landscape scale under multiple future scenarios for mining areas, which is adverse to the identification of ecological conservation regions. This study used the MOP-PLUS (multi-objective optimization problem and patch-level land use simulation) model to simulate the land use patterns in the balance of ecology and economy (EEB) scenario and ecological development priority (EDP) scenario for the Shendong coal base. Then, climate change and land use patterns were integrated into ecosystem models to analyze the dynamic changes in the ecological networks. Finally, the conservation priorities were constructed, and dynamic conservation hotspots were identified using landscape mapping methods. The following results were obtained: (1) From 2000 to 2020, large grassland areas were replaced by mining areas, while cultivated land was replenished. By 2030, the forest and grassland areas (967.00 km^2, 8989.70 km^2) will reach their peaks and the coal mine area (356.15 km^2) will reach its nadir in the EDP scenario. (2) The fragmentation of ecological sources intensified (MPS decreased from 19.81 km^2 to 18.68 km^2) and ecological connectivity declined (in particular, α decreased by 6.58%) from 2000 to 2020. In 2030, the connectivity in the EDP scenario will increase, while the connectivity in the EEB scenario will be close to that of 2020. (3) The central and southeastern parts of the Shendong coal base have higher conservation priorities, which urgently need to be strengthened. This study offers guidance on addressing the challenges of habitat and biodiversity conservation in mining areas.

Keywords: ecological networks; climate change; dynamic conservation; open-pit coal mining; multi-scenario prediction

check for updates

Citation: Zhang, W.; Jiang, Z.; Dai, H.; Lin, G.; Liu, K.; Yan, R.; Zhu, Y. Modelling Multi-Scenario Ecological Network Patterns and Dynamic Spatial Conservation Priorities in Mining Areas. *Land* **2024**, *13*, 1065. https://doi.org/10.3390/land13071065

Academic Editor: Nir Krakauer

Received: 21 June 2024
Revised: 12 July 2024
Accepted: 14 July 2024
Published: 16 July 2024

Copyright: © 2024 by the authors. Licensee MDPI, Basel, Switzerland. This article is an open access article distributed under the terms and conditions of the Creative Commons Attribution (CC BY) license (https://creativecommons.org/licenses/by/4.0/).

1. Introduction

According to the International Energy Agency (IEA) report, China's coal production hit a new high in 2020 (3764 million tons), accounting for 50% of the world's coal production [1]. As the proportion of open-pit coal mines in China's coal industry has gradually increased, its open-pit coal production has become the second largest in the world [2,3]. The entire lifecycle of open-pit mining, from construction to mining and processing, exerts a profound impact on the surface environment, including vegetation removal, land

occupation, and topographical alteration, thereby changing the original pattern of the land use significantly [4–6]. As open-pit mining areas expand, the abundant ecological land resources are progressively replaced, exacerbating the fragmentation of the landscape [7]. The habitats of numerous flora and fauna have suffered irreversible destruction due to the loss of their living environment, resulting in a severe threat to biodiversity [8–10].

An ecological network (EN) is a dispersed habitat network connected by different types of ecological nodes. Based on landscape ecology theory, it is essential component for protecting habitat connectivity and mitigating fragmentation in ecosystems [11,12]. ENs originated from urban beautification in the 18th century, and today, they have gradually evolved towards repairing fragmented habitats and species habitats, enhancing the ecological service functions of ENs [13,14]. Ecological sources, as one of the key elements of ENs, possess high ecological service and species habitat values [15]. Meanwhile, ecological corridors, another important element, reduce the island effect by connecting multiple fragmented species habitats [16,17]. Many studies have adopted various methods to extract the two types of elements. For the identification of ecological sources, there are primarily two methods: (1) The direct identification method—Natural or near-natural patches such as forests or parks are viewed directly as ecological sources. However, this method overlooks the actual contributions of the internal quality and the connectivity between patches. (2) The indicator assessment method—landscape connectivity, ecological sensitivity, and habitat importance are common identification indexes [18,19]. For the identification of ecological corridors, there are primarily three methods: (1) Animal monitoring and tracking—By monitoring and tracking animal migration and combining species dispersal models, a network structure can be constructed. However, this method is time-consuming and requires high-quality data. (2) Minimum Cumulative Resistance (MCR)—It takes into account the source, distance, and basic resistance characteristics. This approach has certain advantages in nature reserves with high ecological stability and is widely used [20,21]. However, in ecologically fragile areas, densely populated regions, and urban agglomerations, it often overlooks the existing structural corridors within a landscape and their relationships with other landscape elements [19,22]. (3) Circuit theory—This method sees the species migration and ecological processes within a landscape as electrical currents, fully considering the randomness of species movement and the redundancy of corridors. It is widely used [23,24]. After the construction of an EN, it is necessary to evaluate the connectivity effectiveness. Common methods include empirical analysis, landscape pattern indices, network structure indices such as the gravity model method, and the connectivity indices method based on graph theory [25,26]. Through these analyses, the relationships and actions between ecological elements can be revealed and the structural characteristics and functional relationships of environmental benefits can be identified. An EN provides a reference for accurately guiding spatial management and conservation.

However, existing studies about EN construction usually focus on specific time slices, paying more attention to current status descriptions and static analysis. They lack in-depth explorations of dynamic evolution and provide weak predictive guidance for the development of regional ENs [27]. It is crucial to assess the landscape changes under ecosystem disturbances, as this helps to understand the adaptability and resilience in the face of multiple future scenarios [28]. Based on the future landscape patterns, targeted interruption measures can be made to reduce the pressure of mining activities on biodiversity. Additionally, recent studies have pointed out that focusing solely on static landscape priorities may overlook habitats that are crucial for ecosystem connectivity, resulting in ineffective regional conservation measures and a waste of financial resources [29]. Therefore, accurately pinpointing the change hotspots within the EN is a key step in enhancing the effectiveness and pertinence of protection measures.

Although ENs have become a common approach in the field of land use management, in-depth discussions in mining areas remain relatively scarce. The rapid change in land use caused by mining has led to habitat fragmentation and loss and a decline in biodiversity and ecological function connectivity [5]. Even so, currently, most studies in mining area

ecology are limited to the assessment of material properties of single elements such as soil, vegetation, and waterbodies [30–32]. Although there are landscape studies in some mining areas, they rely solely on ecosystem service value (ESV) coefficients, with only a few employing biophysical models for quantitative analysis [33,34].

This study constructed multi-scenario ENs based on land use patterns, and then assessed the dynamic changes in the EN under the disturbances of mining activities and climate change. In addition, protection priorities were identified, and a 3 × 3 km grid priority protection strategy was proposed. The main contents of this study are as follows: (1) The spatiotemporal changes in land use in the Shendong coal base (SD) from 2000 to 2030 were simulated using the MOP-PLUS model. (2) ENs were constructed using landscape graph methods, and the dynamic changes in the EN were analyzed based on multi-scenario land use patterns. (3) The protection priorities of EN elements and hotspot changes were assessed and identified, and spatial protection strategies were proposed. This study provided reference for mining areas to take targeted regional protection measures in advance, thereby avoiding the failure of protection and the waste of funds.

2. Materials and Methods

2.1. Study Area

The Shendong coal base (SD) has the largest coal production and is the most important thermal coal export base in China, as its open-pit mining output accounts for approximately 18% of the country's total. The SD is located in the transitional zone of Inner Mongolia, Shanxi, and Shaanxi province, with an area of 14,816.08 km^2 (Figure 1). It covers the northern edge of the Loess Plateau and the transitional zone to the eastern part of the Mu Us Desert, and it has a temperate arid and semi-arid continental monsoon climate, with an annual precipitation of about 400 mm and an annual average evaporation of about 1300 mm [35]. The study area is characterized by gullies and fragmented surfaces. Large-scale open-pit coal mines have strongly disturbed the fragile ecological environment, further intensifying the tension between energy-dependent economic development and the demands of environmental protection. With the transformation of the original ecological landscape, natural habitats are subjected to degradation and loss [36].

2.2. Materials and Pre-Processing

Firstly, land use patterns for SD were simulated by the MOP-PLUS model in the ecological development priority (EDP) scenario and the balance of ecology and economy (EEB) scenario of 2030. Secondly, the habitat suitability and resistance surfaces were conducted using landscape factors from 2000 to 2030, and ecological network of SD was constructed. Thirdly, ecological sources, ecological corridors, and network connectivity were used to assess multi-temporal analysis of ecological network elements. Finally, spatial conservation grids were identified, and spatial protection strategies were proposed in SD (Figure 2).

Land use, road network, socioeconomic datasets, natural datasets, and topographic datasets were the inputs of the MOP-PLUS model to simulate land use layout in 2030. Land use, soil datasets, and the SSP-RCP dataset were the inputs of the InVEST model (water yield, habitat quality, sediment delivery ratio, carbon storage) to construct habitat suitability and resistance surfaces. Dataset (1) mainly includes six types (cultivated land, forest, grassland, waterbody, construction land, and unused land). In this study, open-pit coal mines were identified by manual visual interpretation, and original land use was covered with the coal mines. Finally, seven types were obtained; (2) includes five types of data used for calculating available plant water content, soil erosion factor, and constructing carbon pools [37]; (3) was used to extract freeway, railway, national highway, provincial roads, and country roads for threat sources from construction; (4) includes POP, GDP, and industry output value. POP and GDP were driving factors of the MOP-PLUS model, and the industry output value was the parameter of constraint condition of land use quantity [38]; (5) includes precipitation and evaporation data. The precipitation data were

the driving factor of the MOP-PLUS model, and evaporation data were used to calculate sediment delivery ratio; (6) are SSP-RCP prediction datasets. The dataset is a comprehensive system that takes into account social dynamics, economic trends, environmental conditions, and policy directions, predicting potential future scenarios arising from the interaction of human activities and climate change [39]. In this study, the EDP scenario used the SSP1-1.9 prediction dataset, while the EEB scenario used the SSP2-4.5 prediction dataset; (7) was used to extract watersheds and topographic position index (TPI). The TPI is an important index to describe relief and topography. The accuracy of the data is ensured by comparing the remote sensing image with the actual historical image and investigating the relevant research. See Table 1 for detailed description.

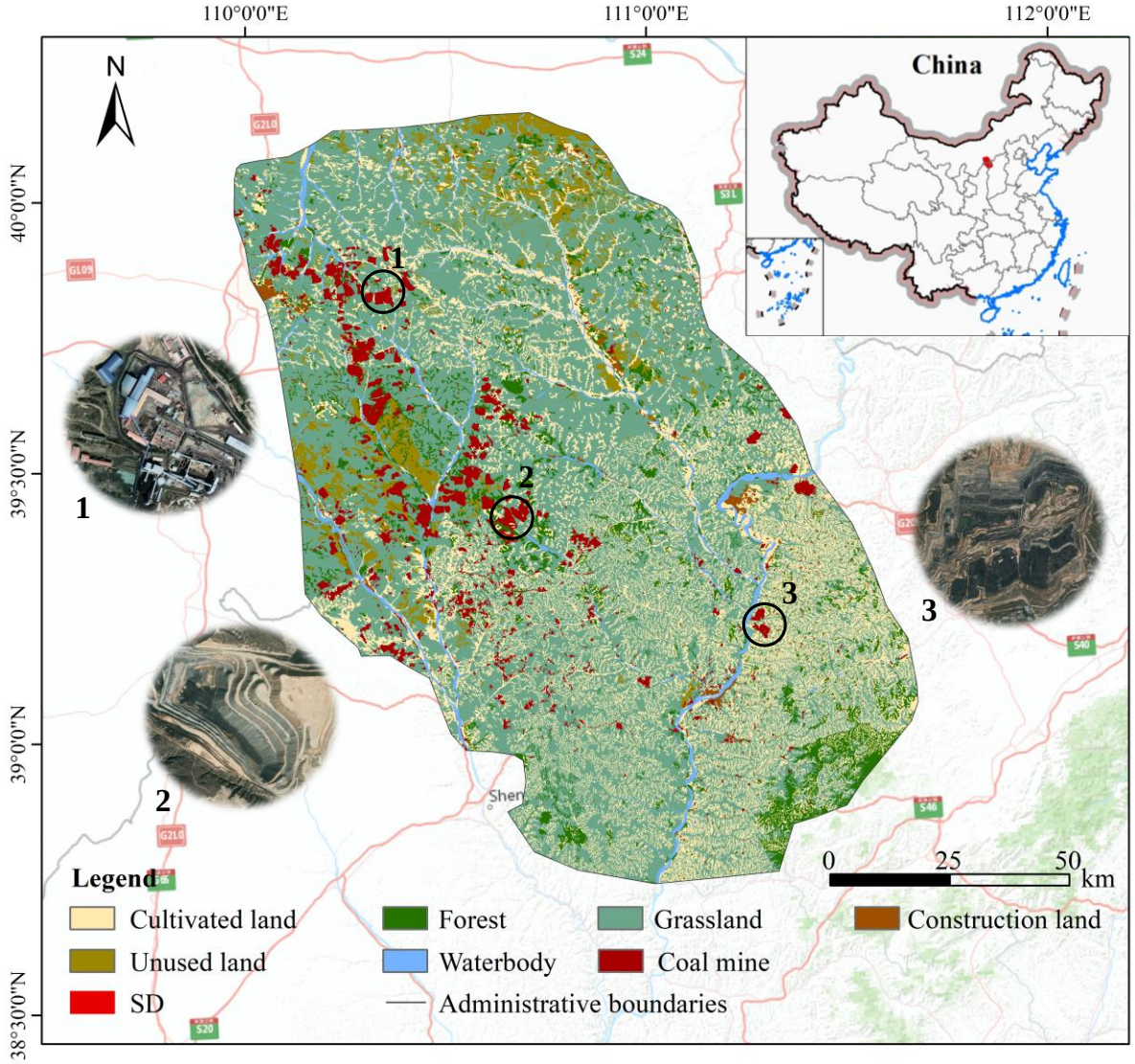


Figure 1. The geographical location of the SD and open-pit mining images.

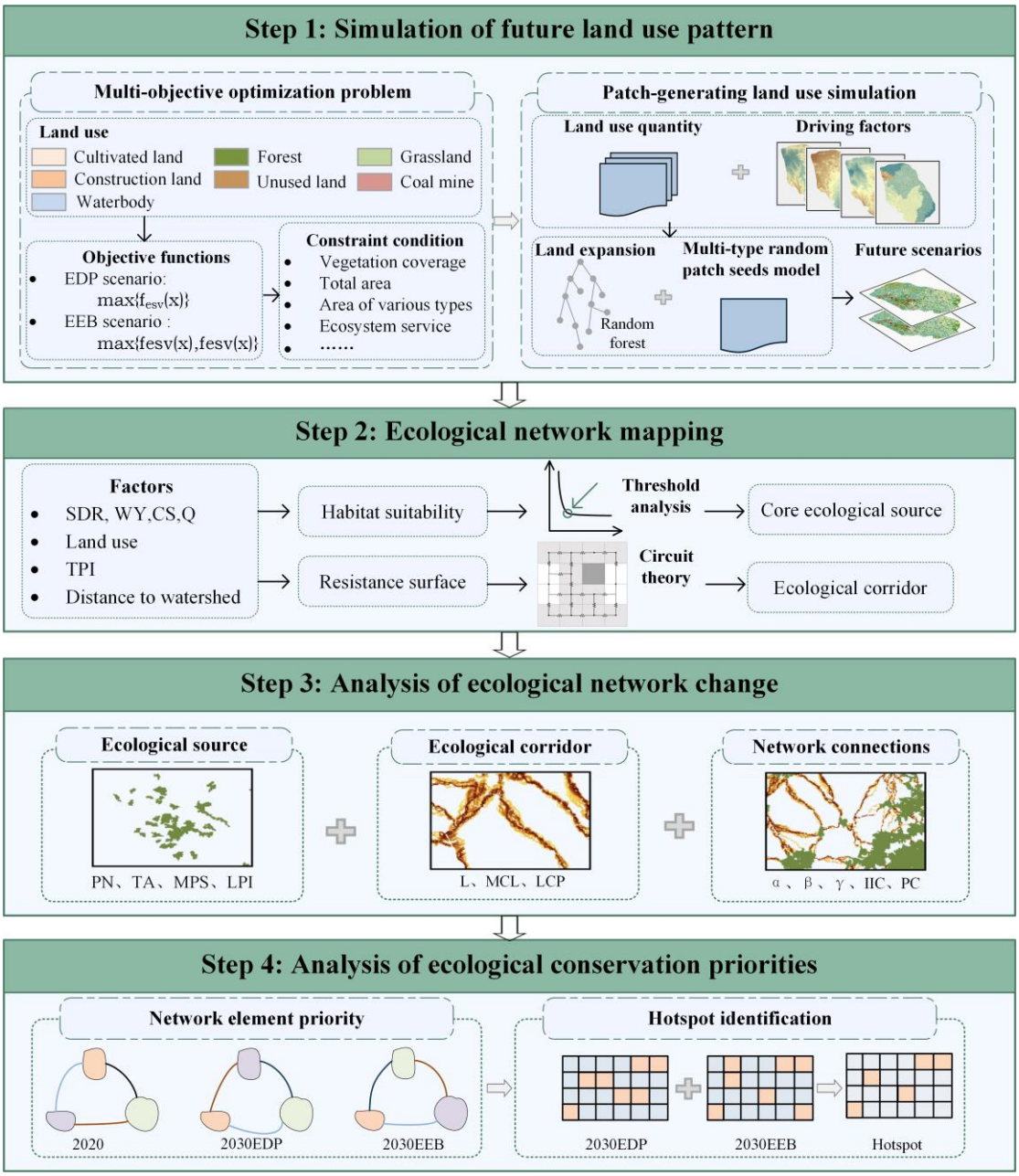


Figure 2. The four main parts and their process framework.

2.2.1. Land Use Simulation

Land Use Demand Assessment Based on MOP Model

Currently, the contradiction between economic development and environmental protection in SD is becoming increasingly apparent. This study took the balance between the two as its starting point and designed two scenarios: the EDP and EEB scenario. With reference to relevant planning and statistical data, ten constraints were designed to determine the land use demands in 2030 under each scenario (Table 2)

Table 1. Datasets and sources.

Datasets	No.	Data	Source	Unit	Resolution	Processing
Land use	(1)	Land use data	Resource and Environmental Science Data Platform (https://www.resdc.cn/DOI/DOI.aspx?DOIID=54) (accessed on 15 April 2024)	--	30 m	
Soil datasets	(2)	Harmonized World Soil Database	Geographic Data Sharing Infrastructure, College of Urban and Environmental Science, Peking University (http://geodata.pku.edu.cn) (accessed on 15 April 2024)	--	1 km	Calculating available plant water content and soil erosion factor [40]
		Depth to bedrock	http://globalchange.bnu.edu.cn/research/cdtb.jsp (accessed on 15 April 2024)	m	1 km	--
		Aboveground/subsurface biological carbon density	(Spawn and Gibbs, 2020) (https://doi.org/10.3334/ORNLDAAC/1763) (accessed on 15 April 2024)	Mg/ha	300 m	Building carbon pool
		Soil surface organic carbon density	Global Soil Organic Carbon Map v1.5 (http://54.229.242.119/GSOCmap) (accessed on 18 April 2024)	T/ha	1 km	Building carbon pool
Road network	(3)	Freeway Railway National highway Provincial roads Country roads	Open Street Map (https://www.openstreetmap.org/) (accessed on 18 April 2024)	-	---	Building threat sources
Socioeconomic datasets	(4)	POP	Resource and Environmental Science Data Platform (https://www.resdc.cn) (accessed on 18 April 2024)	people/km^2	1 km	Drivers of the PLUS model
		GDP		10^4 CNY/km^2	1 km	
		Industry output value	Statistic Yearbook	10^4 CNY	--	Predicting the pattern of land use
Natural datasets	(5)	Precipitation	National Earth System Science Data Center (https://www.geodata.cn/data) (accessed on 18 April 2024)	0.1 mm	1 km	Calculating the annual precipitation and rainfall erosivity [41]
		Evaporation		0.1 mm	1 km	Calculating the annual evaporation
SSP-RCP prediction datasets	(6)	Precipitation prediction dataset	A Big Earth Data Platform for Three Poles (https://poles.tpdc.ac.cn/zh-hans/data/) (accessed on 22 April 2024)	0.1 mm	1 km	Calculating the water yield and sediment delivery ratio
		Evaporation prediction dataset	National Tibetan Plateau Data Center (https://www.tpdc.ac.cn/zh-hans/data/70a3ad6b-9847-476d-a11e-a493d6c31af1) (accessed on 22 April 2024)	m/day	0.25°	Calculating the sediment delivery ratio
Topographic dataset	(7)	DEM	Geospatial Data Cloud (https://www.gscloud.cn/) (accessed on 22 April 2024)	m	30 m	Extracting watersheds, calculating TPI

Table 2. The setting of the MOP model.

Parameter Type	No.	Description	Equation
Decision variables	--	The area of land use	$x_i, i = 1, 2, \ldots, 7$
Objective function	--	EDP	$\max\{f_{esv}(x)\}, f_{esv}(x) = \sum_{i=1}^{7} esv_i \times x_i$
	--	EEB	$\max\{f_{eb}(x), f_{esv}(x)\}, f_{eb}(x) = \sum_{i=1}^{7} eb_i \times x_i$
	(1)	Total area	$\sum_{i=1}^{7} x_i = 14816.08, x_i > 0$
	(2)	Vegetation coverage	$0.46x_1 + x_2 + 0.49x_3 \geq 14816.08 \times 50\%$
	(3)	Cultivated land	$3329.72 \leq x_1 \leq 3598.36$
	(4)	Forest	$x_2 \geq 967.39$
	(5)	Grassland	$8466.38 \times (1 - 5\%) \leq x_3 \leq 8466.38 \times (1 + 5\%)$
	(6)	Waterbody	$373.99 \leq x_4 \leq 389.39$
	(7)	Construction land	$165.66 \leq x_5 \leq 177.70$
	(8)	Unused land	$536.69 \leq x_6 \leq 673.71$
	(9)	Coal mines	$589.32 \times 30\% \leq x_6 \leq 589.32 \times 60\%$
	(10)	Ecosystem service value	$164x_1 + 1645x_2 + 756x_3 + 2837x_4 + 0.27x_6 \geq 9589560.90$

The EDP focuses on restoring and protecting the ecological environment, optimizing ecosystem functions, and maximizing ecosystem service value (ESV). According to Costanza et al. [42] on global ecosystem services, the formula is as follows (unit: 10^4 CNY/km^2):

$$f_{esv}(x) = 164x_1 + 1645x_2 + 756x_3 + 2837x_4 + 0.27x_6 \quad (1)$$

The EEB aims to achieve a trade-off between increased economic benefits and improved ecological functions by adjusting the land structure to maximize economic benefits and ecosystem services. Drawing on the methods of previous studies, the economic value is calculated using industry output values [43,44]. The output value of each industry is converted from the statistical yearbooks of Inner Mongolia, Shaanxi, and Shanxi Province in equal proportion to the area of the SD; the formula is as follows:

$$f_{eb}(x) = 534521.90x_1 + 32028.74x_2 + 303842.00x_3 + 5161.22x_4 + 3105593.00x_5 + 5019595.00x_7 \quad (2)$$

The rules for the 10 constraints were as follows: (1) The area of each land use type was greater than zero, and the total area was 14,816.08 km^2. (2) Based on the vegetation coverage rate at the national level and a certain ecological restoration advance demonstration area in the SD in 2020, it was determined that the vegetation coverage rate in the SD will be at least 50% in 2030. This was calculated using the green equivalent method [44]. (3) Under the basic premise of maintaining national and regional stability, the plan to return farmland to forests and grasslands emphasized by the National Development and Reform Commission (https://www.ndrc.gov.cn/fggz/fgjh/jsxy/202006/t20200604_1230371.html) (accessed on 25 April 2024) in 2020 will be effectively implemented. Therefore, the lower limit was the area of cultivated land with a slope of less than 6° for three consecutive periods, and the upper limit was the area of cultivated land in 2020. (4) As this policy is just starting to be implemented, the increase in forest area over the next 10 years should exceed the pace of the past; therefore, the area was set to be larger than the current trend (the prediction result from the Markov chain model was 967.39 km^2). (5) Since 2000, the grassland area has been in a relatively stable state, with small fluctuations. Therefore, based on the 2020 grassland area, the change was limited to 5%. (6) SD is located in the arid desert area, and the shortage of water resources is very serious. This phenomenon is exacerbated by the decline in the water table due to coal mining. Therefore, the lower limit was set as the area from the Markov chain (373.99 km^2), and the upper limit was the maximum value in the three periods. (7) The lower limit was set as the area in 2020, and the upper limit was the area from the Markov chain (177.70 km^2). (8) Unused land can be reclaimed for construction land and

ecological land. Therefore, the lower limit was set as the minimum area in the three periods, and the upper limit was the area of unused land in 2020. (9) Based on mine information extracted from the National Energy Administration, as of 2020, there were 39 abandoned open-pit mines and 101 producing open-pit mines in the SD (https://www.nea.gov.cn/) (accessed on 25 April 2024). It is planned that all abandoned mines will be ecologically restored by 2030, and the vegetation coverage rate will reach 100%. The lower limit was 30% of the 2020 mine area, and the upper limit was 60%. (10) In the new ecological protection strategy, soil and water conservation and other engineering measures in the SD are given high priority. Therefore, the lower limit was the ecosystem service value in 2020 (http://video.yrcc.gov.cn/zwzc/zcjd/202403/t20240314_427419. html) (accessed on 25 April 2024).

Land Use Pattern Simulation Based on PLUS Model

The PLUS model was developed by Liang et al. [45] based on the CA-MarKov, CLUE-S, and FLUS models in combination with the random forest model. This model integrates land expansion analysis based on the random forest model and multi-type random patch seed mechanisms based on the CA model, including both the LEAS and CARS modules. The LEAS module adopts the random forest classification method to study the relationships between the growth and driving factors of different land use types in order to obtain the probability of development for each land use type. The CARS module simulates land use distribution patterns by determining the development probabilities of different land use types.

In this study, 2020 was the base year, and the EEB and EDP scenarios were used to simulate land use in 2030. The driving factors included temperature (T), precipitation (P), DEM, GDP, POP, distance to a coal mine, distance to water, distance to a freeway, distance to a railway, distance to a national highway, distance to a provincial road, and distance to a county road (Figure 3). The land use pattern in 2020 was simulated based on the land use patterns in 2000 and 2010, and the overall accuracy and Kappa coefficient were used for accuracy evaluation.

2.2.2. Ecological Network Construction

Core Ecological Source Identification

Ecological sources are key land patches that exert significant influence over the ecological dynamics and functions within a region. Based on existing research, in this study, land use type, ecosystem services (ESs), the topography position index (TPI), and distance to a watershed were chosen as key ecological factors to evaluate the habitat suitability of the raster data [46].

A patch with an ecological source score greater than 75 was chosen as a potential ecological source. Then, the threshold analysis method was used to select core ecological sources. Setting the minimum area of the patches during the identification of core ecological sources directly affected the number of patches. As the minimum threshold increased, the patch number decreased rapidly. After the threshold was increased to 2 km^2, the patch number tended to level off, so the minimum area threshold of the patches was set to 2 km^2. The ecological source score was from 0 to 100, with scores closer to 100 indicating higher habitat suitability and scores closer to 0 indicating lower habitat suitability.

Resistance Surface Construction

Constructing ecological resistance surfaces scientifically is more conducive to identifying major areas for ecological protection. Different types of natural landforms affect the distributions and activities of species, as well as the exchange of matter, energy, and information [47]. Worse still, human construction activities also hinder species migration and the benign development of ecological sources [48]. This study combined the natural background and the development degree, then selected the land use type, the TPI, the importance of ESs, and the distance to a watershed as resistance factors for land use, terrain,

habitats, and human activity interference, respectively [46] (Table 3). The resistance score ranges from 0 to 1000, with scores closer to 1000 indicating higher resistance and scores closer to 0 indicating lower resistance [49,50]. For example, waterbody blocks species migration and the resistance score exhibits a maximum value of 1000.

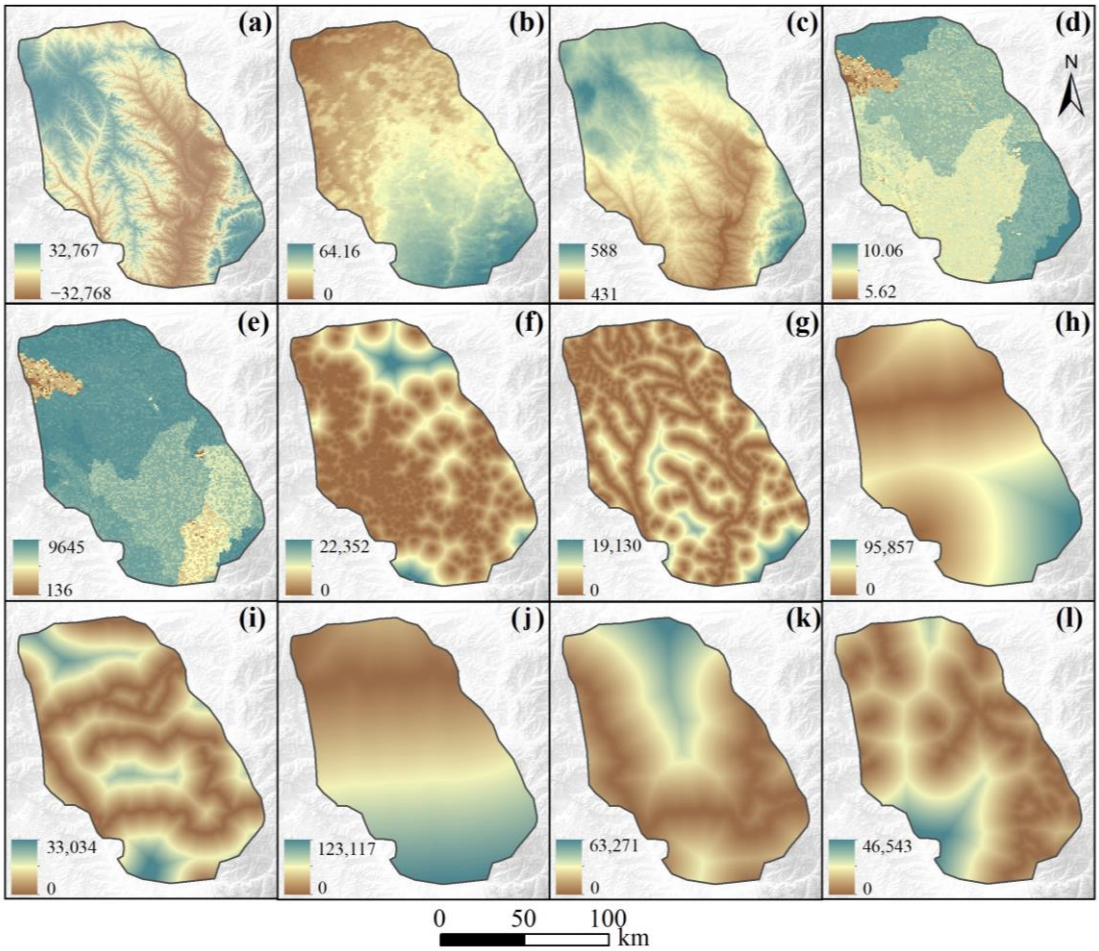


Figure 3. Driving factors of PLUS model. (**a**) DEM (m); (**b**) P (mm); (**c**) T (°C); (**d**) GDP (1×10^4 CNY/km^2); (**e**) POP (per/km^2); (**f**) distance to coal mines (m); (**g**) distance to water (m); (**h**) distance to freeway (m); (**i**) distance to railway (m); (**j**) distance to national highway (m); (**k**) distance to provincial roads (m); (**l**) distance to county roads (m).

Table 3. Ecological source score and resistance score.

Category	Content	Ecological Source Score	Resistance Score
Land use type	Cultivated land	50	200
	Forest	100	1
	Grassland	80	50
	Water bodies	0	1000
	Construction land	0	500
	Unused land	20	10
	Coal mine	0	600
Ecosystem services (ES)	0–0.25	60	100
	0.25–0.41	80	50
	0.41–0.70	100	1

Table 3. *Cont.*

Category	Content	Ecological Source Score	Resistance Score
Topography position index (TPI)	Ridge	10	800
	Abrupt slope	30	300
	Gentle slope	50	200
	Gorge	90	10
Distance to watershed	0–1 km	100	10
	1–3 km	90	50
	3–5 km	70	100
	5–10 km	60	200
	10–184 km	30	300

Ecological Corridor Extraction

A resistance surface is a reflection of trends in ecological flow movement and the migration choices of species. It aims to quantify the degree of hindrance in species dispersion. Drawing on the method of circuit theory, ENs equate ecological resistance with electrical resistance and analogizes ecological flows (migration and energy transfer) to electric current [24,51]. Based on circuit theory, this study combined core ecological sources and resistance surfaces to construct least-cost pathways as optimal corridors for species movement between in situ sites.

2.2.3. Analysis of Ecological Network Change

Analysis of Core Ecological Source

The indicators used for the analysis of changes in the core ecological source mainly included four aspects: the patch number (PN), total area (TA), mean patch size (MPS), and largest patch index (LPI). The PN and TA reflect the abundance of the core ecological source. Enough habitats can support the coexistence of different species, which is important for ecosystem stability [52,53]. The MPS reflects the evenness of species distribution, where a larger MPS indicates higher species diversity [54]. The LPI reflects the dominant patch type in the landscape [54]. See Table 4 for detailed formulas and descriptions.

Table 4. Ecological network index.

Content	Index	References
Core ecological source	PN	[55]
	TA (km^2)	[52]
	MPS (km^2)	[54]
	LPI (%)	[54]
Ecological corridor	L	[55]
	MCL (km)	[55]
Network connectivity	α	[56]
	β	[57]
	γ	[58]
	IIC	[59]
	PC	[60]

Analysis of Ecological Corridor

The number of ecological corridors (L) and mean corridor length (MCL) were used to analyze the change in the ecological corridors in 2000, 2020, and 2030. A greater number of ecological corridors usually reflects better ecosystem connectivity and a greater potential for species movement and exchange between different ecological sources. The MCL reflects the ability of ecological corridors to connect different ecological sources. The larger the MCL, the more detrimental it is to species migration [55]. See Table 4 for detailed formulas and descriptions.

Analysis of Network Connectivity

Based on ENs composed of the core ecological source and ecological corridor, network connectivity was evaluated based on two aspects: structural connectivity and functional connectivity. The structural connectivity indices of an ecological network include network circuitry (α), the line point rate (β), and network connectedness (γ). The corridor was evaluated using connectivity and circularity indices. α is the ratio of the actual loop number in a network to the maximum possible loop number in ENs, representing the degree of possible pathways for species migration [56]. β is also the network circularity index, which measures how easy it is for a node in a network to connect to other nodes [57]. γ is the ratio of corridor numbers to the maximum possible number, representing the overall complexity of the network connectivity [58].

The functional connectivity indices include the integral index of connectivity (IIC) and the probability of connectivity (PC). The larger the IIC, the higher the degree of connectivity between habitat patches [59]. The larger PC, the greater probability of connectivity [60]. See Table 4 for detailed formulas and descriptions.

2.2.4. Analysis of Conservation Priorities

This study analyzed the conservation priorities based on two aspects: ENs and landscape patterns. In terms of ENs, the conservation priorities of the core ecological sources were determined based on betweenness centrality [61]. Betweenness centrality is the number of shortest paths through the nodes in ENs. Corridor conservation priorities were calculated based on linkage priority using the Linkage Mapper tool. This tool took into account a weighted combination of many factors, such as shape, size, average resistance values, and expert opinion. In terms of landscape patterns, the mean values of habitat suitability, resistance surfaces, and corridor centrality were calculated for 2020 and 2030 (EEB and EDP scenarios) based on 3 km $\times$ 3 km grids. The values in 2020 were subtracted from those of the two scenarios in 2030, and the grids where the results were all negative were areas with high priority for landscape conservation.

3. Results

3.1. Spatiotemporal Land Use Variations in SD

Using land use data from 2000 and 2010 to predict 2020, the overall accuracy of the model was 0.86 and the Kappa coefficient was 0.76, proving that the model accurately simulated the spatial suitability of land growth. Figure 4 shows the distributions of land use patterns in 2000, 2020, and 2030 (EEB and EDP scenarios). The land use types in the SD were primarily grassland and cultivated land, accounting for more than 80% of the total area, with the highest proportion in 2000 at 86.30%. Unused land was mainly distributed in the northeastern and western parts of the area. From 2000 to 2020, the areas of coal mines increased sharply to 4.04% (598.57 km^2), mainly in the northwestern part (Areas 1 and 2 in Figure 4). Under the EEB and EDP scenarios, the areas of coal mines were predicted to decrease by 181.81 km^2 and 242.17 km^2, respectively. From 2000 to 2030, the area of cultivated land gradually decreased, with the reduction percentages being 2.45% and 3.41% under the two scenarios. In contrast, forest and grassland were predicted to reach their peak in the EDP scenario, accounting for 67.20%. Intensive forest land was consistently distributed in the southeastern part (Area 3 in Figure 4).

Figure 5 shows the land use conversion from 2000 to 2020 and from 2020 to 2030 (EEB and EDP scenarios). The total areas of land use conversion for the three periods were 1720.00 km^2, 227.90 km^2, and 691.77 km^2, respectively. From 2000 to 2020, the land use conversion was dominated by grassland to coal mines (404.94 km^2), cultivated land to grassland (254.09 km^2), and cultivated land to coal mines (116.71 km^2). Under the EDP scenario, coal mines will be ecologically restored, with 40.31% of the area being converted into forests and grassland, exceeding the conversion rate in the EEB scenario by 10.30%. However, in the EDP scenario, more unused land will be converted into grassland, resulting

in the lowest area of unused land, at 71.07 km^2. Additionally, there were varying degrees of land use transfer in forests, construction land, and waterbodies.

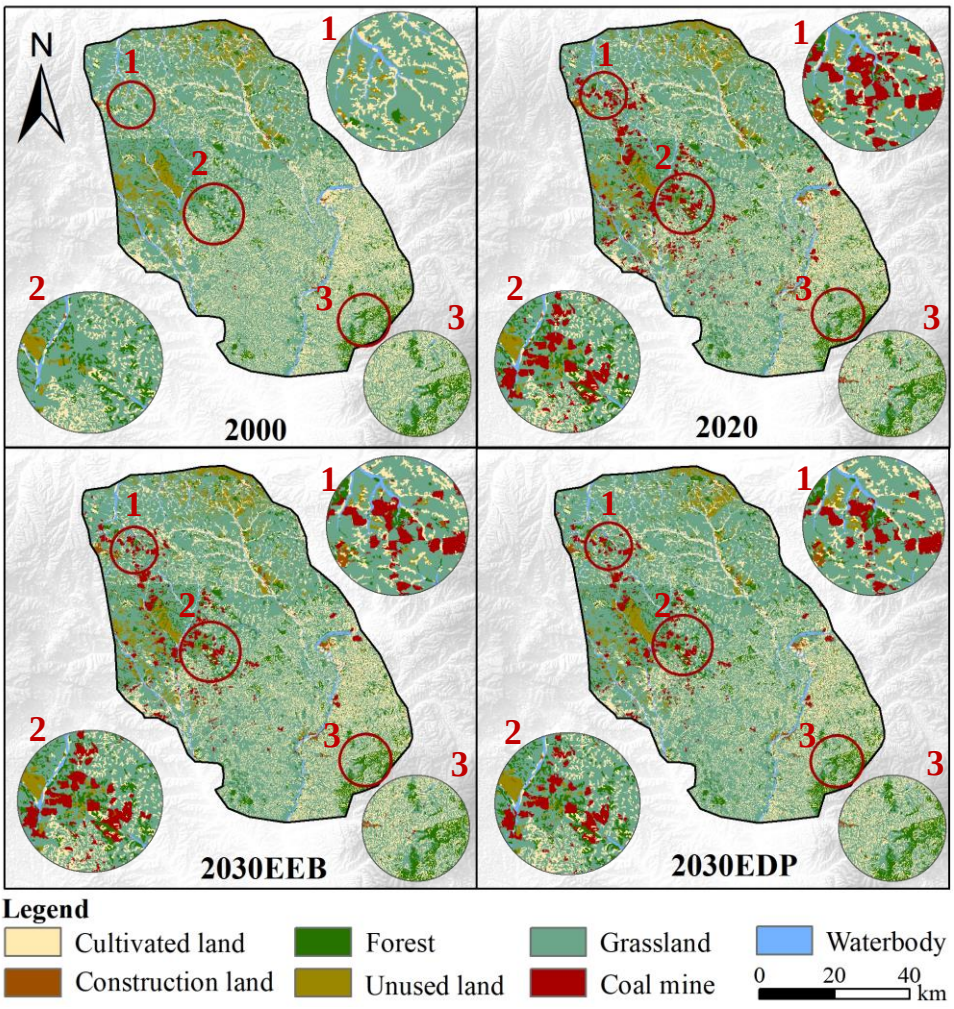


Figure 4. Distributions of land use patterns in 2000, 2020, and 2030 (EDP and EEB scenarios).

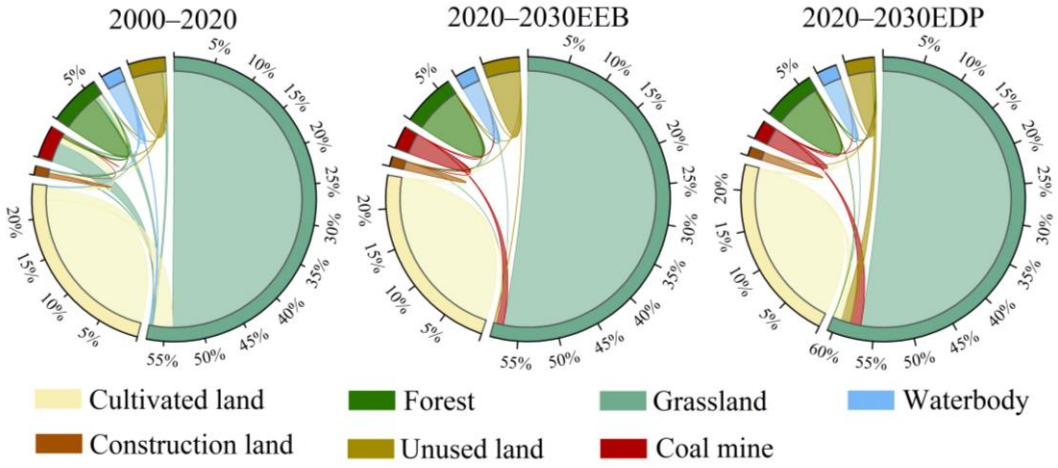


Figure 5. Land use transfers from 2000 to 2020, and from 2020 to 2030 (EDP and EEB scenarios).

3.2. Spatiotemporal Variation of ENs in SD

3.2.1. Spatiotemporal Variation in Habitat Suitability

Figure 6 shows the spatial distributions of habitat suitability in the SD for 2000, 2020, and 2030 under two scenarios. Habitat suitability was high in the southern and central regions (due to the extensive forest distribution) and low in the western and northeastern regions (due to widespread coal mines and unused land). The average habitat quality of the SD decreased from 77.12 to 76.21 from 2000 to 2020, and the proportion of highly suitable areas (levels 4 and 5) also decreased from 59.63% to 58.32%. Under the EEB scenario, the proportion of level 1 will significantly decrease and the combined proportion of suitable areas (levels 3, 4, and 5) will increase by 11.68% compared to those in 2000 and 12.77% compared to those in 2020, reaching a total of 81.78%. Under the EDP scenario, the proportion of highly suitable areas will reach the highest level in history (60.22%) and the proportion of level 1 will reach the lowest.

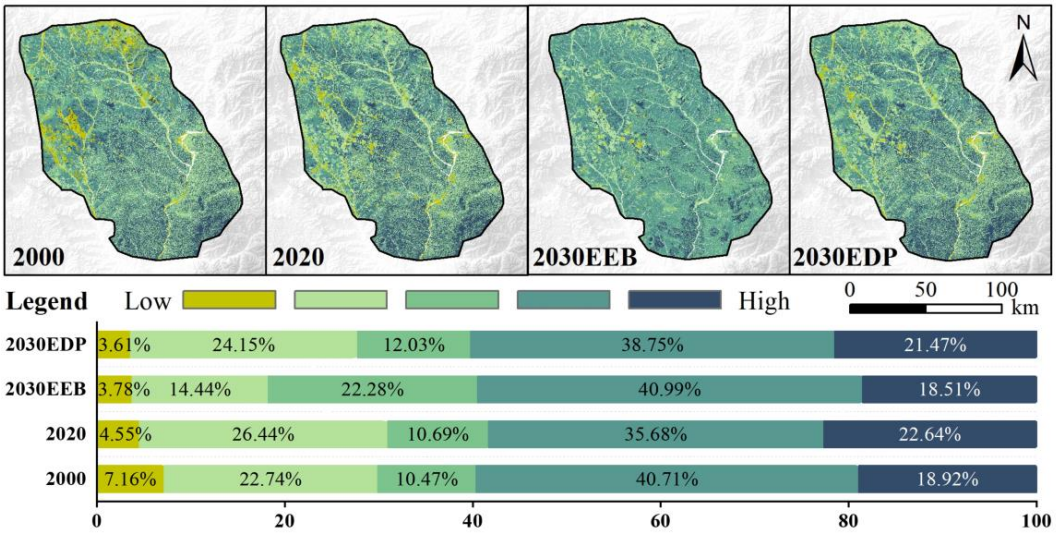


Figure 6. Distributions of habitat suitability in 2000, 2020, and 2030 (EEB and EDP scenarios).

3.2.2. Spatiotemporal Variation in Resistance Surface

Figure 7 shows the spatial distributions of resistance surfaces in the SD for 2000, 2020, and 2030 under two scenarios. High-resistance regions (levels 4 and 5) were primarily distributed in the unused land and coal mines, while low-resistance regions (level 1) were mainly distributed in the north of the SD. From 2000 to 2020, the proportion with high resistance increased by 2.52%, with the main increase occurring in the coal mines in the northwestern part. Under the EEB and EDP scenarios, high-resistance areas are expected to decrease by 1.17% and 2.54%, respectively, compared to those in 2020, while low-resistance areas are expected to decrease by 8.64% and 7.66%, respectively.

3.2.3. Spatiotemporal Variation in ENs

Figure 8 shows the distributions of the EN in 2000, 2020, and 2030 (EEB and EDP scenarios). It indicated that small ecological sources were concentrated in the middle region, while large ecological sources were predominantly located in the southern part. The sudden increase in open-pit mining areas in the west led to the disappearance of small core ecological sources, resulting in a lack of connectivity in the northwestern part of the SD (Area 2 in Figure 8). The ecological source in the central part shrank from 2000 to 2020, and the degree of fragmentation intensified, while the number of ecological corridors increased (Area 1 in Figure 8). Under the EEB scenario, the number of ecological sources and corridors will be approximately the same as in 2020, but the area of the central ecological source will significantly expand. Under the EDP scenario, both the number of core ecological sources and the number of ecological corridors are expected to increase. The small ecological

sources that disappeared in the western part will be restored (Area 2 in Figure 8), and the ecological sources in the southeast will also expand (Area 3 in Figure 8).

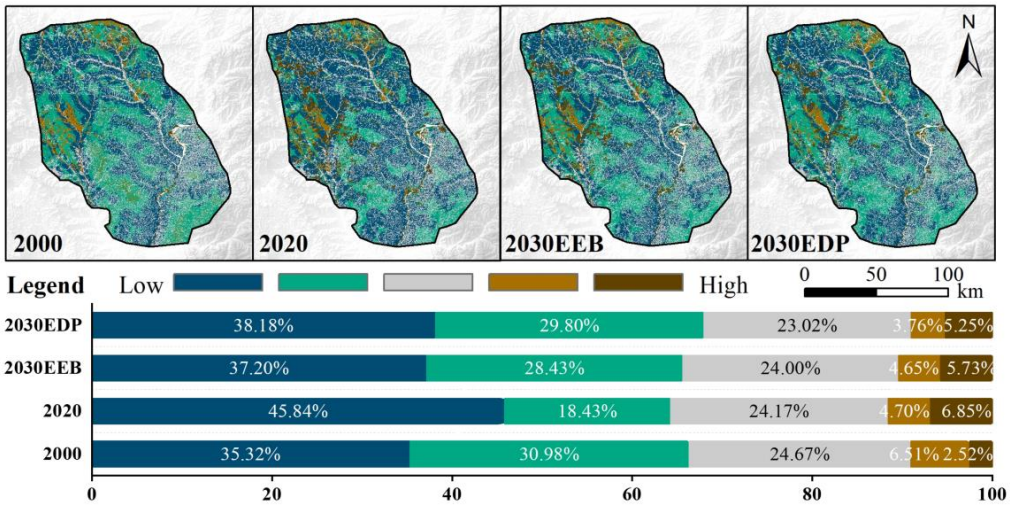


Figure 7. Distributions of resistance surfaces in 2000, 2020, and 2030 (EEB and EDP scenarios).

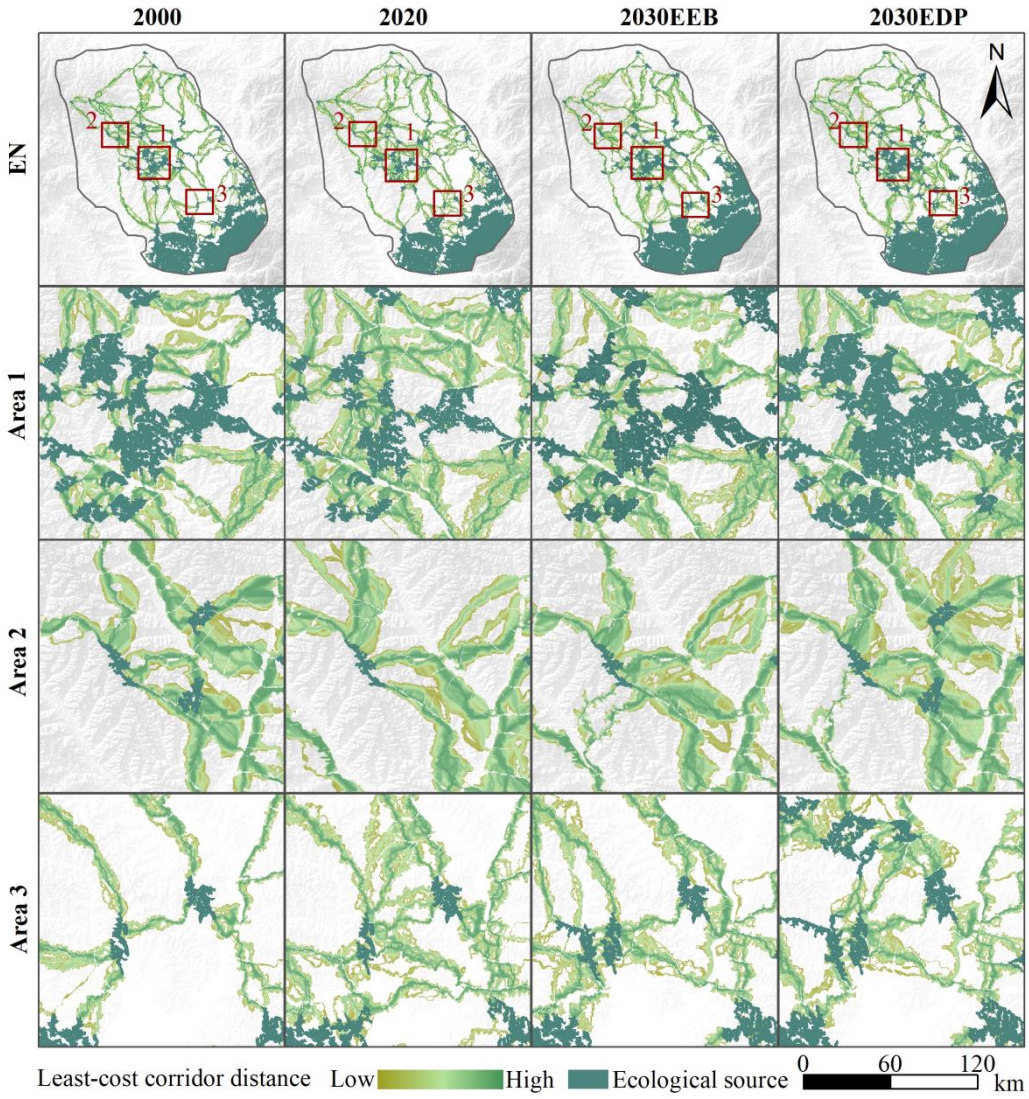


Figure 8. Distribution of ENs in 2000, 2020, and 2030 (EEB and EDP scenarios).

3.2.4. Changes in ENs in SD

Table 5 shows the indicators of the core ecological sources, ecological corridors, and network connectivity for the years 2000, 2020, and 2030 (EED and EDP scenarios). The PN and TA indicated that the number of core ecological sources increased from 81 to 85 between 2000 and 2020, but the total area decreased from 1604.99 km^2 to 1587.83 km^2, with the main changes occurring in the middle region of the SD. The MPS and LPI also showed decreasing trends, indicating the loss and fragmentation of ecological sources. From 2020 to 2030, under both scenarios, the PN and TA both showed increasing trends, and the EDP scenario showed more obvious trends. However, the EDP scenario had smaller MPS and LPI values, indicating more serious fragmentation.

The L and MCL values indicated that the number of ecological corridors increased. Due to habitat fragmentation, there were increases from 200 in 2000 to 212 in the EEB scenario and to 269 in the EDP scenario. The increase in connectivity was attributed to an increase in potential movement paths between ecological sources. The MCL decreased from 11.45 km^2 in 2000 to 10.14 km^2 in 2020 and then increased to 12.15 km^2 in the EEB scenario and decreased to 9.27 km^2 in the EDP scenario. A smaller MCL is more conducive to species migration.

Based on the network connectivity indicators, the values of α, β, γ, IIC, and PC for the year 2000 were the highest among the four periods. The ecological network in 2000 had the highest physical structural connectivity and functional connectivity. The values for 2020 were essentially similar to those for 2030 under both the EEB and EDP scenarios.

Table 5. Indicators for ecological network elements in 2000, 2020, and 2030 (EED and EDP scenarios).

Content	Indicators	2000	2020	2030EEB	2030EDP
Core ecological source	PN	81	85	91	111
	TA (km^2)	1604.99	1587.83	1799.72	2133.09
	MPS (km^2)	19.81	18.68	19.78	19.22
	LPI (%)	44.24	43.23	41.41	36.62
Ecological corridor	L	200	201	212	269
	MCL	11.45	10.14	12.15	9.27
Network connectivity	α	0.76	0.71	0.69	0.73
	β	2.47	2.36	2.34	2.42
	γ	0.84	0.81	0.79	0.82
	IIC	0.21	0.20	0.21	0.21
	PC	0.38	0.36	0.36	0.36

3.3. Ecological Conservation Priorities in SD

Figure 9 shows the conservation priorities for EN elements and landscape hotspots. In 2020, the ecological corridor conservation priority was relatively high in the northwestern and middle regions of the SD. Under the EEB and EDP scenarios, the ecological corridor priorities were generally lower compared to 2020. The betweenness centrality of the ecological source in the EEB scenario was similar to that in 2020. However, in the EDP scenario, there was a significant increase in the betweenness centrality in the central part, with multiple patches being upgraded to the highest level. From 2020 to 2030, the number of ecological corridors with the highest conservation priority in the southeastern region gradually increased. This region has become more densely populated, leading to habitat fragmentation, and its corridors are characterized by the highest or second highest priority.

Based on the 3 km $\times$ 3 km hotspot map, the landscape hotspots generally showed a dense spatial pattern in the central and southeastern regions, which was basically consistent with the priorities of the EN. This was mainly reflected in regions with increasing populations (Areas 1 and 2 in Figure 9) and on the edges of the ecological sources (Areas 3 and 4 in Figure 9), especially at the junctions of the sources and corridors.

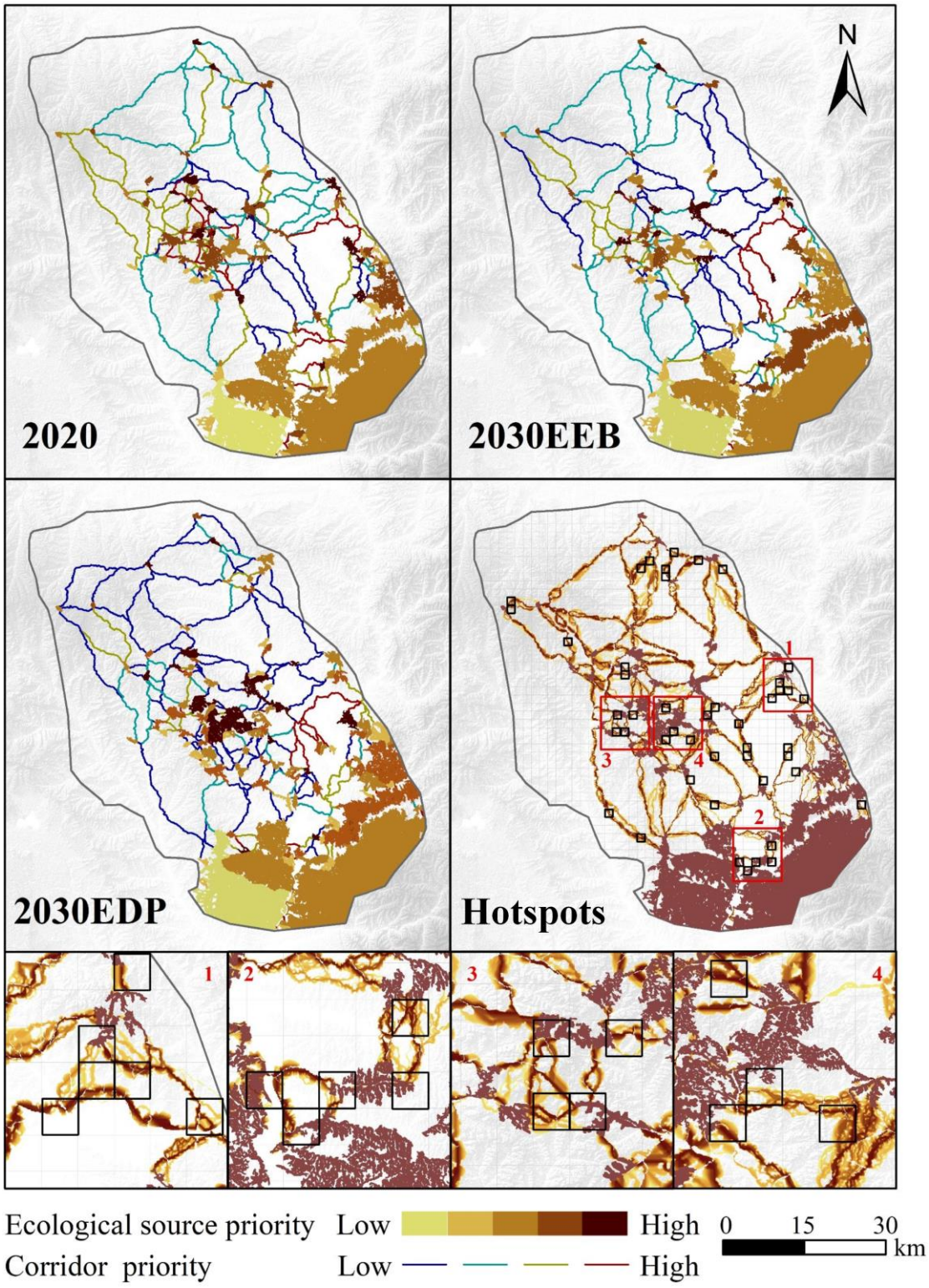


Figure 9. Spatial distribution of ecological conservation priorities.

4. Discussion

4.1. The Response of EN in the EEB and EDP Scenarios

As coal resources were being exhausted in eastern China, the 12th Five-Year Plan shifted the focus of coal development to the western regions (https://www.nea.gov.cn/) (accessed on 25 April 2024). The coal production of Inner Mongolia, Shaanxi, Shanxi, and Xinjiang Province increased to 69% of the national total in 2017 and then increased to 77.75%

by 2020 (https://www.nea.gov.cn/) (accessed on 25 April 2024). The SD, as the largest coal reserve area in China, plays a significant role in the planning. Additionally, the SD occupies a transitional region, bridging a cultivated zone with a pastoral zone, and land use has further exacerbated the degradation and fragmentation of both natural and improved ecosystems [5]. This study indicated that the area of coal mines surged, growing from 11.11 km^2 to 598.28 km^2 from 2000 to 2020. Ecological sources were gradually occupied by coal mines, leading to the shrinkage of patches. Moreover, continuous areas were divided into new patches, resulting in an increase in ecological sources. Under the EDP scenario, ecological connectivity will be improved, which will correlate with a significant increase in the area to 2133.09 km^2, with 524.38 km^2 of grassland contributing the most to this increase.

It is widely believed that industrialization has exacerbated regional habitat fragmentation and reduced the accessibility of habitats [62,63]. However, the EEB scenario in this study indicated that mitigation of industrialization may not necessarily lead to the recovery of connectivity. While the mining area is expected to decrease by 181.76 km^2, this is not sufficient to offset the impact of fragmentation on the ecological background of the SD. The number of ecological sources will increase from 85 to 91, with most being small patches. However, the number of corridors will only increase slightly from 201 to 212, which means that the connections between the newly added patches will not correspondingly increase. As a result, the overall connectivity of the EN will not improve effectively. Furthermore, Gao et al. [46] also found results contrary to common sense in Wuhan urban agglomeration. His study indicated that the development of urbanization did not necessarily lead to a reduction in connectivity, which was related to the increase in grassland. Therefore, in areas with intense industrial activities and urban expansion, strategies should be adopted that are tailored to the specific ecological characteristics and social context. This study suggests that strengthening bioremediation and soil remediation and using other technologies for integrated management to improve the ecosystem's self-repairing ability could improve this situation of high fragmentation and low connectivity in the SD.

However, even though the EDP scenario can bring ecological benefits, such as increasing core habitats and landscape connectivity, this does not mean that it is always considered the best choice. Actual decisions require a balance of various factors, including economic costs, social needs, political considerations, and the overall strategy for regional development [64]. While the EEP scenario contributes to long-term environmental health and biodiversity, it may impact economic growth and employment opportunities in the short term, especially in areas that rely on traditional mining. Therefore, policy makers need to find a balance between ecological protection and economic development [65]. Additionally, based on the high landscape fragmentation of the ecological background in the SD, the development of the EDP scenario will overlook the details of local variations, specifically in the southeastern part of the SD. It is projected that by the year 2030, the increasing ecological sources will lead to more severe landscape fragmentation.

4.2. Spatial Conservation Priority of EN in SD

The core ecological sources and ecological corridors were prioritized into five and four levels, respectively (Figure 9). The higher conservation priorities of the SD were mainly in the central and northwestern parts. This was due to the dense and scattered distribution patterns of the coal mines in these regions. In 2020, the development of the mining industry resulted in increased resistance, leading to the ecological corridors being classified as the highest and second highest levels, placing them in a critical protection position. Ecological corridors, as bridges between different ecological sources, have an irreplaceable role in facilitating the flow of matter, energy, and information. Prioritizing the protection of these ecological corridors is critical to maintaining the flow of overall ecological functions. From 2020 to 2030, after ecological protection and management, the priorities of the central and northwestern ecological corridors will be significantly alleviated. Under the EDP scenario, the increase in the betweenness centrality of the central sources will be related to the increase in habitat fragmentation. These sources will gradually evolve into stepping

stones connecting the large sources in the southeast. Additionally, it is projected that by 2030, the number of top-level ecological corridors in the southeastern part will increase due to the increasing population density. An increasing population brings greater ecological challenges such as urban heat island effects [66,67]. Ecological corridors promote ecosystem connectivity and integrity by connecting urban green spaces and parks. Additionally, they also play essential roles in maintaining biodiversity, promoting ecological processes, and improving the urban environment.

Hotspot identification was performed based on landscape method. This analysis considered the landscape values within a 3 × 3 km grid, and the grids where the landscape values decreased in both scenarios are displayed in Figure 9. The results indicated that the hotspots were mainly distributed in the central and southeastern regions. These hotspots had a trend of increasing ecological risk and required targeted ecological protection efforts. The landscape hotspots were mainly concentrated at the junctions of ecological sources and ecological corridors, as well as areas with increasing population density. This result was consistent with Gao et al. [46]. These junctions are ecological buffer zones that balance the impacts of actions such as restoring cultivated lands to forests and grassland, and mining activities. They need to be given adequate attention.

4.3. Limitations

Based on changes in land use, this study explored the EN and conservation hotspots of the SD from 2000 to 2020 and in 2030, but there were some limitations. (1) This study did not consider planned open-pit coal mines after 2020, so it lacked the impact of newly built coal mines on land use patterns in future years. (2) Only four key ecosystem services were selected in this study, but services such as air quality regulation and noise regulation are equally important to mining areas. In the future, it will be necessary to have more detailed survey data of the coal mines and more comprehensive ecosystem assessment to enhance the scientific validity of this research.

5. Conclusions

This study took into account the impacts of mining activities and climate change to explore the changes in the EN of the SD from 2000 to 2020 and the projected year 2030 under the EEB and EDP scenarios, including ecological source areas, ecological corridors, and network connectivity. Then, the priorities of EN elements from 2020 to 2030 were calculated and hotspots of landscape change were identified. The spatial distribution of the EN indicated that small ecological sources were densely distributed in the middle region, while large ecological sources were distributed in the southeastern region. The density of the ecological corridors was high in the center and decreased in the surrounding areas. The EN changes indicated that from 2000 to 2020, the ecological sources shrank and ecological connectivity decreased, while the numbers of ecological sources and corridors increased. Under the EDP scenario, connectivity will increase, while under the EEB scenario, connectivity will be close to that in 2020. The EN conservation priorities indicated that corridors and sources in the central and northwestern parts have higher priorities. This is due to the mining industry, which has increased the resistance to development in these areas. Under the EDP scenario, the conservation priorities will be effectively alleviated. The hotspots were mainly distributed at the junctions of the central ecological sources and corridors, as well as in the increasingly populated southeastern region. By identifying landscape hotspots, it is possible to effectively avoid blind protection and to coordinate conflicts between ecological conservation and economic development. However, we do not only emphasize areas with high landscape priority; we also need to pay more attention to the hotspots of landscape change, especially the areas where were reduced. Taking preemptive ecological protection measures in these hotspot areas can help prevent the failure of conservation efforts and the waste of funds. In addition, bioremediation and soil remediation technologies should be strengthened to improve the self-healing ability of ecosystems and assist artificial restoration to restore landscape connectivity.

Author Contributions: W.Z.: Writing—review and editing, Writing—original draft, Methodology, Investigation, Formal analysis, Visualization, Conceptualization. Z.J.: Writing—review and editing, Conceptualization, Software. H.D.: Writing—review and editing, Conceptualization. G.L.: Conceptualization, Formal analysis, Funding acquisition, Writing—review and editing. K.L.: Conceptualization, Validation, Writing—review and editing. R.Y.: Writing—review and editing, Methodology, Conceptualization. Y.Z.: Writing—review and editing, Methodology. All authors have read and agreed to the published version of the manuscript.

Funding: This research was supported by the National Natural Science Foundation of China (Grant No. 42103079 and 42202280).

Data Availability Statement: Data will be made available on request.

Conflicts of Interest: The authors declare no conflicts of interest.

References

1. IEA. Coal2021-Analysis and Forecast to 2024. International Energy Agency. 2021. Available online: https://www.oecd-ilibrary.org/energy/coal-2021_ba0095c1-en (accessed on 25 April 2024).
2. Jia, Z.; Lin, B. How to achieve the first step of the carbon-neutrality 2060 target in China: The coal substitution perspective. *Energy* **2021**, *233*, 121179. [CrossRef]
3. Jiang, W.; Sun, Y. Which is the more important factor of carbon emission, coal consumption or industrial structure? *Energy Policy* **2023**, *176*, 113508. [CrossRef]
4. Dou, S.; Xu, D.; Keenan, R.J. Effect of income, industry structure and environmental regulation on the ecological impacts of mining: An analysis for Guangxi Province in China. *J. Clean. Prod.* **2023**, *400*, 136654. [CrossRef]
5. Wang, Z.; Luo, K.; Zhao, Y.; Lechner, A.M.; Wu, J.; Zhu, Q.; Sha, W.; Wang, Y. Modelling regional ecological security pattern and restoration priorities after long-term intensive open-pit coal mining. *Sci. Total Environ.* **2022**, *835*, 155491. [CrossRef] [PubMed]
6. Wu, Z.; Lei, S.; Yan, Q.; Bian, Z.; Lu, Q. Landscape ecological network construction controlling surface coal mining effect on landscape ecology: A case study of a mining city in semi-arid steppe. *Ecol. Indic.* **2021**, *133*, 108403. [CrossRef]
7. Duan, X.; Chen, Y.; Wang, L.; Zheng, G.; Liang, T. The impact of land use and land cover changes on the landscape pattern and ecosystem service value in Sanjiangyuan region of the Qinghai-Tibet Plateau. *J. Environ. Manag.* **2023**, *325*, 116539. [CrossRef] [PubMed]
8. Iván, L.; Irene, C.; Isaías, R.; Virginia, N. Mining threatens health of Panama's environment. *Science* **2023**, *382*, 1007–1008. [CrossRef]
9. Kong, X.; Fu, M.; Zhao, X.; Wang, J.; Jiang, P. Ecological effects of land-use change on two sides of the Hu Huanyong Line in China. *Land Use Policy* **2022**, *113*, 105895. [CrossRef]
10. Yan, Y.; Jarvie, S.; Liu, Q.; Zhang, Q. Effects of fragmentation on grassland plant diversity depend on the habitat specialization of species. *Biol. Conserv.* **2022**, *275*, 109773. [CrossRef]
11. Luo, Y.; Wu, J.; Wang, X.; Zhao, Y.; Feng, Z. Understanding ecological groups under landscape fragmentation based on network theory. *Landsc. Urban Plan.* **2021**, *210*, 104066. [CrossRef]
12. Wu, Z.; Cheng, S.; Xu, K.; Qian, Y. Ecological network resilience evaluation and ecological strategic space identification based on complex network theory: A case study of Nanjing city. *Ecol. Indic.* **2024**, *158*, 111604. [CrossRef]
13. De Montis, A.; Caschili, S.; Mulas, M.; Modica, G.; Ganciu, A.; Bardi, A.; Ledda, A.; Dessena, L.; Laudari, L.; Fichera, C.R. Urban–rural ecological networks for landscape planning. *Land Use Policy* **2016**, *50*, 312–327. [CrossRef]
14. Jakiel, M.; Bernatek, A. *Assessment of an Ecological Network at Local Scale in the Context of Landscape Changes: A Case Study from NE Poland, In Landscape Analysis and Planning: Geographical Perspectives*; Luc, M., Somorowska, U., Szmańda, J.B., Eds.; Springer International Publishing: Cham, Switzerland, 2015; pp. 245–256. [CrossRef]
15. Yu, Q.; Yue, D.; Wang, J.; Zhang, Q.; Li, Y.; Yu, Y.; Chen, J.; Li, N. The optimization of urban ecological infrastructure network based on the changes of county landscape patterns: A typical case study of ecological fragile zone located at Deng Kou (Inner Mongolia). *J. Clean. Prod.* **2017**, *163*, S54–S67. [CrossRef]
16. Wade, A.A.; Mckelvey, K.S.; Schwartz, M.K. Resistance-surface-based wildlife conservation connectivity modeling: Summary of efforts in the United States and guide for practitioners. *USDA For. Serv.-Gen. Tech. Rep.* **2015**, *333*, 1–93. [CrossRef]
17. Pierik, M.E.; Dell'Acqua, M.; Confalonieri, R.; Bocchi, S.; Gomarasca, S. Designing ecological corridors in a fragmented landscape: A fuzzy approach to circuit connectivity analysis. *Ecol. Indic.* **2016**, *67*, 807–820. [CrossRef]
18. Hong, W.; Guo, R.; Su, M.; Tang, H.; Chen, L.; Hu, W. Sensitivity evaluation and land-use control of urban ecological corridors: A case study of Shenzhen, China. *Land Use Policy* **2017**, *62*, 316–325. [CrossRef]
19. Yang, L.; Li, Y.; Jia, L.; Ji, Y.; Hu, G. Ecological risk assessment and ecological security pattern optimization in the middle reaches of the Yellow River based on ERI+MCR model. *J. Geogr. Sci.* **2023**, *33*, 823–844. [CrossRef]
20. Yang, C.; Guo, H.; Huang, X.; Wang, Y.; Li, X.; Cui, X. Ecological network construction of a national park based on MSPA and MCR models: An example of the proposed national parks of "Ailaoshan-Wuliangshan" in China. *Land* **2022**, *11*, 1913. [CrossRef]

21. Ma, J.; Yu, Q.; Wang, H.; Yang, L.; Wang, R.; Fang, M. Construction and optimization of wetland landscape ecological network in Dongying City, China. *Land* **2022**, *11*, 1226. [CrossRef]
22. Hu, C.; Wang, Z.; Wang, Y.; Sun, D.; Zhang, J. Combining MSPA-MCR Model to Evaluate the Ecological Network in Wuhan, China. *Land* **2022**, *11*, 213. [CrossRef]
23. Gao, C.; Pan, H.; Wang, M.; Zhang, T.; He, Y.; Cheng, J.; Yao, C. Identifying priority areas for ecological conservation and restoration based on circuit theory and dynamic weighted complex network: A case study of the Sichuan Basin. *Ecol. Indic.* **2023**, *155*, 111064. [CrossRef]
24. Zhou, G.; Huan, Y.; Wang, L.; Lan, Y.; Liang, T.; Shi, B.; Zhang, Q. Linking ecosystem services and circuit theory to identify priority conservation and restoration areas from an ecological network perspective. *Sci. Total Environ.* **2023**, *873*, 162261. [CrossRef] [PubMed]
25. Li, J.; Chen, Y.; Peng, H.; He, L. Dynamic rule of ecological risk transmission among ecological communities based on network environmental analysis. *Sci. Total Environ.* **2021**, *781*, 146729. [CrossRef]
26. Zhang, R.; Zhang, L.; Zhong, Q.; Zhang, Q.; Ji, Y.; Song, P.; Wang, Q. An optimized evaluation method of an urban ecological network: The case of the Minhang District of Shanghai. *Urban For. Urban Green.* **2021**, *62*, 127158. [CrossRef]
27. Valainis, U.; Balalaikins, M.; Soms, J.; Bastyte-Cseh, D.; Gintaras, A.; Baneliene, A.; Augutis, D.; Zukovskiene, M.; Nitcis, M.; Zolovs, M. Ecological network for species dependent on ancient broadleaf trees using Osmoderma barnabita as a model species: A new approach. *Insect Conserv. Divers.* **2022**, *15*, 273–287. [CrossRef]
28. Wang, X.; Yonghong Li, F.; Zhang, J.; Liu, J.; Wang, Y.; Guo, Y.; Baoyin, T.; Liu, X. Changes in plant and arthropod functional traits mediate land use and precipitation effects on grassland production. *Ecol. Indic.* **2022**, *135*, 108535. [CrossRef]
29. Bishop-Taylor, R.; Tulbure, M.G.; Broich, M. Evaluating static and dynamic landscape connectivity modelling using a 25-year remote sensing time series. *Landsc. Ecol.* **2018**, *33*, 625–640. [CrossRef]
30. Li, S.; Wang, J.; Zhang, M.; Tang, Q. Characterizing and attributing the vegetation coverage changes in North Shanxi coal base of China from 1987 to 2020. *Resour. Policy* **2021**, *74*, 102331. [CrossRef]
31. Liu, X.; Shi, H.; Bai, Z.; Zhou, W.; Liu, K.; Wang, M.; He, Y. Heavy metal concentrations of soils near the large opencast coal mine pits in China. *Chemosphere* **2020**, *244*, 125360. [CrossRef]
32. Tozsin, G. Hazardous elements in soil and coal from the Oltu coal mine district, Turkey. *Int. J. Coal Geol.* **2014**, *131*, 1–6. [CrossRef]
33. Han, T.; Li, Q.; Hai, Y.; Yang, Y.; Wen, Z.; Li, R.; Zheng, H. Response of ecosystem services and environmental dynamics in large open-pit coal mines: A case study in semi-arid areas. *Glob. Ecol. Conserv.* **2024**, *51*, e02891. [CrossRef]
34. Li, F.; Liu, X.; Zhao, D.; Wang, B.; Jin, J.; Hu, D. Evaluating and modeling ecosystem service loss of coal mining: A case study of Mentougou district of Beijing, China. *Ecol. Complex.* **2011**, *8*, 139–143. [CrossRef]
35. Xu, D.Y.; Kang, X.W.; Zhuang, D.F.; Pan, J.J. Multi-scale quantitative assessment of the relative roles of climate change and human activities in desertification–A case study of the Ordos Plateau, China. *J. Arid Environ.* **2010**, *74*, 498–507. [CrossRef]
36. Zhu, G.P.; Li, H.Q.; Zhao, L.; Man, L.; Liu, Q. Mapping the ecological dimensions and potential distributions of endangered relic shrubs in western Ordos biodiversity center. *Sci. Rep.* **2016**, *6*, 26268. [CrossRef] [PubMed]
37. Bhattacharya, R.K.; Das Chatterjee, N.; Das, K. Modelling of soil erosion susceptibility incorporating sediment connectivity and export at landscape scale using integrated machine learning, InVEST-SDR and Fragstats. *J. Environ. Manag.* **2024**, *353*, 120164. [CrossRef] [PubMed]
38. Shi, Q.; Gu, C.-J.; Xiao, C. Multiple scenarios analysis on land use simulation by coupling socioeconomic and ecological sustainability in Shanghai, China. *Sustain. Cities Soc.* **2023**, *95*, 104578. [CrossRef]
39. Tebaldi, C.; Debeire, K.; Eyring, V.; Fischer, E.; Fyfe, J.; Friedlingstein, P.; Knutti, R.; Lowe, J.; O'Neill, B.; Sanderson, B.; et al. Climate model projections from the Scenario Model Intercomparison Project (ScenarioMIP) of CMIP6. *Earth Syst. Dyn.* **2021**, *12*, 253–293. [CrossRef]
40. Williams, J.R.; Arnold, J.G. A system of erosion—Sediment yield models. *Soil Technol.* **1997**, *11*, 43–55. [CrossRef]
41. Wischmeier, W.H.; Smith, D.D. *Predicting Rainfall Erosion Losses—A Guide to Conservation Planning*; Agriculture Handbook; Department of Agriculture: Washington, DC, USA, 1978.
42. Costanza, R.; d'Arge, R.; De Groot, R.; Farber, S.; Grasso, M.; Hannon, B.; Limburg, K.; Naeem, S.; O'Neill, R.V.; Paruelo, J.; et al. The value of the world's ecosystem services and natural capital. *Nature* **1997**, *387*, 253–260. [CrossRef]
43. Li, C.; Wu, Y.; Gao, B.; Zheng, K.; Wu, Y.; Li, C. Multi-scenario simulation of ecosystem service value for optimization of land use in the Sichuan-Yunnan ecological barrier, China. *Ecol. Indic.* **2021**, *132*, 108328. [CrossRef]
44. Wang, Y.; Li, X.; Zhang, Q.; Li, J.; Zhou, X. Projections of future land use changes: Multiple scenarios-based impacts analysis on ecosystem services for Wuhan city, China. *Ecol. Indic.* **2018**, *94*, 430–445. [CrossRef]
45. Liang, X.; Guan, Q.; Clarke, K.C.; Liu, S.; Wang, B.; Yao, Y. Understanding the drivers of sustainable land expansion using a patch-generating land use simulation (PLUS) model: A case study in Wuhan, China. *Comput. Environ. Urban Syst.* **2021**, *85*, 101569. [CrossRef]
46. Gao, J.; Gong, J.; Li, Y.; Yang, J.; Liang, X. Ecological network assessment in dynamic landscapes: Multi-scenario simulation and conservation priority analysis. *Land Use Policy* **2024**, *139*, 107059. [CrossRef]
47. Zhang, K.; Chen, L.R.; Xu, H.M.; Li, Y.Y. Spatial variability of plant community characteristics and its influencing factors in a small watershed of wind-water erosion crisscross region on the Loess Plateau, China. *Ying Yong Sheng Tai Xue Bao* **2019**, *30*, 2521–2530. [CrossRef]

48. Doherty, T.S.; Hays, G.C.; Driscoll, D.A. Human disturbance causes widespread disruption of animal movement. *Nat. Ecol. Evol.* **2021**, *5*, 513–519. [CrossRef]
49. Gurrutxaga, M.; Lozano, P.J.; del Barrio, G. GIS-based approach for incorporating the connectivity of ecological networks into regional planning. *J. Nat. Conserv.* **2010**, *18*, 318–326. [CrossRef]
50. Song, S.; Xu, D.; Hu, S.; Shi, M. Ecological network optimization in urban central district based on complex network theory: A case study with the Urban Central District of Harbin. *Int. J. Environ. Res. Public Health* **2021**, *18*, 1427. [CrossRef]
51. Wang, Y.; Qu, Z.; Zhong, Q.; Zhang, Q.; Zhang, L.; Zhang, R.; Yi, Y.; Zhang, G.; Li, X.; Liu, J. Delimitation of ecological corridors in a highly urbanizing region based on circuit theory and MSPA. *Ecol. Indic.* **2022**, *142*, 109258. [CrossRef]
52. Kong, F.; Wang, D.; Yin, H.; Dronova, I.; Fei, F.; Chen, J.; Pu, Y.; Li, M. Coupling urban 3-D information and circuit theory to advance the development of urban ecological networks. *Conserv. Biol.* **2021**, *35*, 1140–1150. [CrossRef]
53. Wang, F.; Yu, Q.; Qiu, S.; Xu, C.; Ma, J.; Liu, H. Study on the relationship between topological characteristics of ecological spatial network and soil conservation function in southeastern Tibet, China. *Ecol. Indic.* **2023**, *146*, 109791. [CrossRef]
54. McGarigal, K. *FRAGSTATS: Spatial Pattern Analysis Program for Quantifying Landscape Structure*; U.S. Dept. of Agriculture, Forest Service, Pacific Northwest Research Station: Corvallis, OR, USA, 1995. [CrossRef]
55. Cook, E.A. Landscape structure indices for assessing urban ecological networks. *Landsc. Urban Plan.* **2002**, *58*, 269–280. [CrossRef]
56. Miao, Z.; Pan, L.; Wang, Q.; Chen, P.; Yan, C.; Liu, L. Research on urban ecological network under the threat of road networks—A case study of Wuhan. *Int. J. Geo-Inf.* **2019**, *8*, 342. [CrossRef]
57. Linehan, J.; Gross, M.; Finn, J. Greenway planning-developing a landscape ecological network approach. *Landsc. Urban Plan.* **1995**, *33*, 179–193. [CrossRef]
58. Bunn, A.G.; Urban, D.L.; Keitt, T.H. Landscape connectivity: A conservation application of graph theory. *J. Environ. Manag.* **2000**, *59*, 265–278. [CrossRef]
59. Saura, S.; Pascual-Hortal, L. A new habitat availability index to integrate connectivity in landscape conservation planning: Comparison with existing indices and application to a case study. *Landsc. Urban Plan.* **2007**, *83*, 91–103. [CrossRef]
60. Saura, S.; Torné, J. Conefor Sensinode 2.2: A software package for quantifying the importance of habitat patches for landscape connectivity. *Environ. Model. Softw.* **2009**, *24*, 135–139. [CrossRef]
61. Saura, S.; Rubio, L. A common currency for the different ways in which patches and links can contribute to habitat availability and connectivity in the landscape. *Ecography* **2010**, *33*, 523–537. [CrossRef]
62. Liu, Y.; Xiao, L.; Cheng, Z.; Liu, X.; Dai, J.; Zhao, X.; Chen, J.; Li, M.; Chen, Z.; Sun, Q. Anthropogenic impacts on vegetation and biodiversity of the lower Yangtze region during the mid-Holocene. *Quat. Sci. Rev.* **2023**, *299*, 107881. [CrossRef]
63. Wanghe, K.; Guo, X.; Hu, F.; Ahmad, S.; Jin, X.; Khan, T.U.; Xiao, Y.; Luan, X. Spatial coincidence between mining activities and protected areas of giant panda habitat: The geographic overlaps and implications for conservation. *Biol. Conserv.* **2020**, *247*, 108600. [CrossRef]
64. Cao, S.; Ma, Z.; Liu, Z.; Guo, J.; Yuan, W. Achieving Harmony between the Economy and the Environment. *Habitat Int.* **2023**, *131*, 102733. [CrossRef]
65. Huang, J.; Tang, Z.; Liu, D.; He, J. Ecological response to urban development in a changing socio-economic and climate context: Policy implications for balancing regional development and habitat conservation. *Land Use Policy* **2020**, *97*, 104772. [CrossRef]
66. Li, Y.; Sun, Y.; Li, J.; Gao, C. Socioeconomic drivers of urban heat island effect: Empirical evidence from major Chinese cities. *Sustain. Cities Soc.* **2020**, *63*, 102425. [CrossRef]
67. Min, M.; Lin, C.; Duan, X.; Jin, Z.; Zhang, L. Spatial distribution and driving force analysis of urban heat island effect based on raster data: A case study of the Nanjing metropolitan area, China. *Sustain. Cities Soc.* **2019**, *50*, 101637. [CrossRef]

Disclaimer/Publisher's Note: The statements, opinions and data contained in all publications are solely those of the individual author(s) and contributor(s) and not of MDPI and/or the editor(s). MDPI and/or the editor(s) disclaim responsibility for any injury to people or property resulting from any ideas, methods, instructions or products referred to in the content.